Final Technical Report for Award DE-FG02-05ER41389

A New Electrostatically-Focused, UV HPD for Liquid Xenon:
A Direct Comparison with APD, PMT, SiPM in an Integrated Database
08/15/05– 08/14/07
Prepared by Professor Elena Aprile, P.I.
Department of Physics, Columbia University

Within the scope of the project, a LXe detector and associated gas handling and purification system were set up to study the response of various photodetectors to the VUV Xe light. In particular we tested an Advanced Photonix Large Area Avalanche Photodiode (APD), Silicon Photomultipliers (SiPMs) from two different sources and an Hamamtsu Photonics APD. As part of the XENON Dark Matter project, sponsored by the National Science Foundation, we have accumulated independent knowledge of the response of compact metal channel photomultipliers. At this stage, we conclude that the last are far superior in terms of reliability and performance in a LXe detector environment. More studies are needed with APDs and SiPMs in LXe, taking advantage of the improved performance of these sensors with time. We could not test a hybrid PMT (HPD) since the only available unit on loan from one manufacturer lacked the mechanical stability and was packaged in a form not compatible with LXe purity requirements. Meanwhile, within the XENON collaboration, we are developing with Hamamatsu a hybrid PMT which is named QUPID (Quartz Photon Intensifying Detector) which promises to solve the problems of radioactivity and purity encountered with previous HPDs. We attach to this report two papers which summarize in detail the experimental st-ups, procedures and results obtained with different APDs and SiPMs operated in LXe. We continue our investigations of APDs in view of their potential appication in large arrays for LXe detectors. We intend to publish the results once we complete tests of newly acquired Hamamatsu APDs.

Operation of Avalanche Photodiodes in Liquid Xenon

J. Alvarez, E. Aprile, K.L. Giboni, and L.M.P. Fernandes

Department of Physics, Columbia University, New York, NY 10027, USA

Columbia Astrophysics Laboratory Internal Report

Abstract

The operation of different avalanche photodiodes (APDs) for detection of liquid xenon scintillation was investigated. Quantum efficiencies of 1.08±0.05 and 0.80±0.14 where measured for two APD's provided by *Advanced Photonix Inc.* (API) and *Hamamatsu Photonics*, respectively. Both APD types were found to reach gains above 200, although gains as low as a few tens may prove sufficient to achieve optimum performance. Compared to the API photodiodes, the Hamamatsu APDs used in these tests exhibited poor performance.

I. Introduction

Avalanche photodiodes (APDs) have proven to be a good alternative to photomultiplier tubes (PMTs) in visible and VUV photon detection [1,2]. They are compact, consume small amounts of power, and are simple to operate. Operational characteristics such as high quantum efficiency, fair internal gain and insensitiveness to intense magnetic fields combined with a relatively low response to minimum ionizing particles make them competitive alternatives to PMTs for medium and high-energy physics instrumentation applications. In particular, their negligible radioactivity contamination is attractive for low background experiments based on liquid xenon (LXe), such as direct dark matter searches (XENON [3], ZEPLIN [4]) and the neutrinoless double beta decay search (EXO [5]), where the radio-purity of the photosensors is of critical importance. Their main drawbacks compared to PMTs are their low gains and reduced active areas

We have tested the operation of two types of APDs immersed in LXe. Until now, only API APDs *(Deep-UV series)* [6] presented a spectral response extending down to the VUV region (down to 120 nm). Another attractive quality from this perspective is the capability of to operate in direct contact with LXe (at -100 degrees C) with an estimated quantum efficiency (QE^1) of approximately 1 (as reported in [7]). High quantum efficiency for xenon gas scintillation (centred at 172 nm) was also reported to be about 1.2 [6] and 1.3 ± 0.1 [8]. In a previous work [9], we have used an API UV-series large area APD (LAAPD), mounted on a custom designed ceramic enclosure, and obtained a *QE* of 0.45 for the LXe scintillation (centred at 178 nm).

In this work, we summarize the results obtained with an API Deep-UV LAAPD, mounted in a custom designed ceramic enclosure, as well as with custom made Hamamatsu APDs with enhanced sensitivity in the VUV region. The measurements reported in this paper aim to confirm the high *QE* of the API LAAPD and to evaluate the *QE* of the Hamamatsu APDs at 178 nm, while immersed in LXe.

II. Experimental setup

The LAAPDs were mounted on a PTFE plate placed inside a chamber filled with high purity LXe. A negligibly small-sized ^{241}Am alpha source, deposited on the centre of a stainless steel plate, was placed above the LAAPD surface plane. A schematic drawing of the chamber is shown in Fig. 1. An open bath cooling apparatus with a liquid nitrogen (LN_2) and alcohol mixture was used to condense the xenon gas.

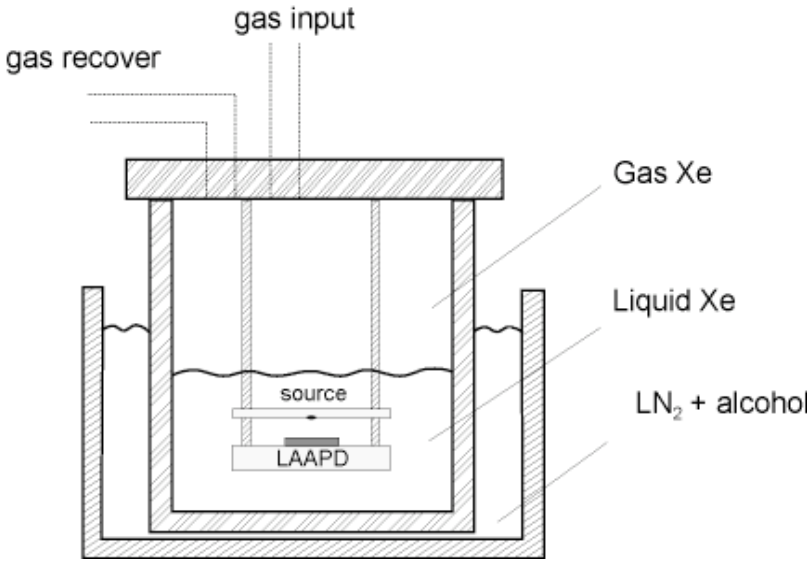

Fig. 1. LAAPD setup for scintillation detection in liquid xenon.

The scintillation light produced by alpha particles absorbed in LXe hits the LAAPD producing electron-hole pairs, which are amplified by avalanche in the silicon. The signal is collected in a charge sensitive preamplifier (*Canberra 2006*) and fed into a low-noise shaping amplifier (*Ortec 450*). Shaping time constants of 250 ns were used in order to optimize the APD performance for detection of the liquid xenon scintillation light, which has two scintillation components decaying at 4.2 ns and 22 ns [10]. The amplified signals are further pulse-height analysed in a multi-channel analyzer (MCA).

Two different types of APDs were tested in the chamber: a circular LAAPD (16 mm diameter) from API, placed in the centre of the PTFE disk, and two square shaped APDs (5×5 mm^2) from Hamamatsu Photonics, placed side by side in the centre of the PTFE plate. The distance between the source plane and the LAAPD surface was 7.5 mm and 6.5 mm for API and Hamamatsu APDs, respectively. With this geometry, the

relative solid angle subtended by the APDs (obtained from a MonteCarlo simulation), is 15.6% for the API LAAPD and 2.35% for each of the Hamamatsu APDs.

Manufacturer	**API**	**Hamamatsu**
Shape	circular, 10mm diam.	square, 5x5 mm^2
Distance from source plane	7.5mm	6.5mm
Fractional solid angle	15.6%	2.35%

The quantum efficiencies of the APDs were estimated by comparison of the VUV-scintillation pulse amplitudes with those resulting from direct interaction of the alpha particles in the photodiodes. The average number of charge carriers produced by alpha particles in the APD can be used as a reference to determine the number of charge carriers produced by the scintillation pulses. The pulse-height distributions from direct interaction of alpha particles in the APDs were obtained when the chamber was kept under vacuum.

III. Results and discussion

A) API LAAPD

Typical pulse-height distributions for direct alpha particles and LXe scintillation detected in the LAAPD are shown in Fig. 2 (a) and (b), respectively. The peaks resulting from direct interaction of alpha particles present a Gaussian shape with negligible tails in the low energy region. This behavior is consistent with the negligible energy loss of the alpha particles in the APD entrance dead layer; alpha particles impinging the APD at different angles lead to essentially the same energy absorbed in the APD.

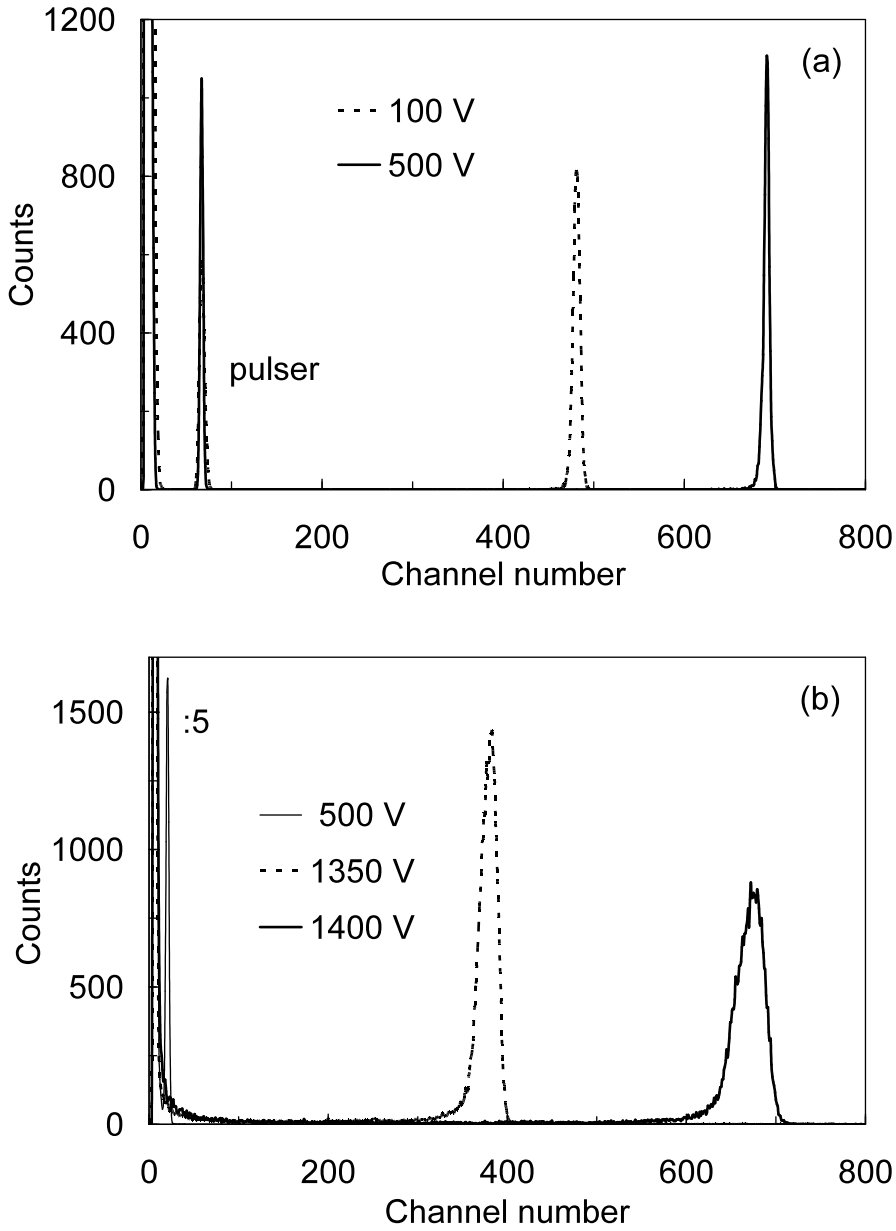

Fig. 2. Pulse-height distributions for direct alpha particles (a) and LXe scintillation (b) detected in the API LAAPD for different bias voltages. For higher bias voltages, alpha particle signals saturate the APD.

Fig. 3 shows the APD gain and energy resolution as a function of APD bias voltage, determined from the pulse-height distributions obtained for VUV scintillation produced in LXe by alpha particles. The unitary gain was obtained for a range of bias voltages around 500 V and is in accordance with the measurements made for visible light pulses from a LED. As shown in Fig. 3, the lowest energy resolution of 5.0% is obtained for gains above 35.

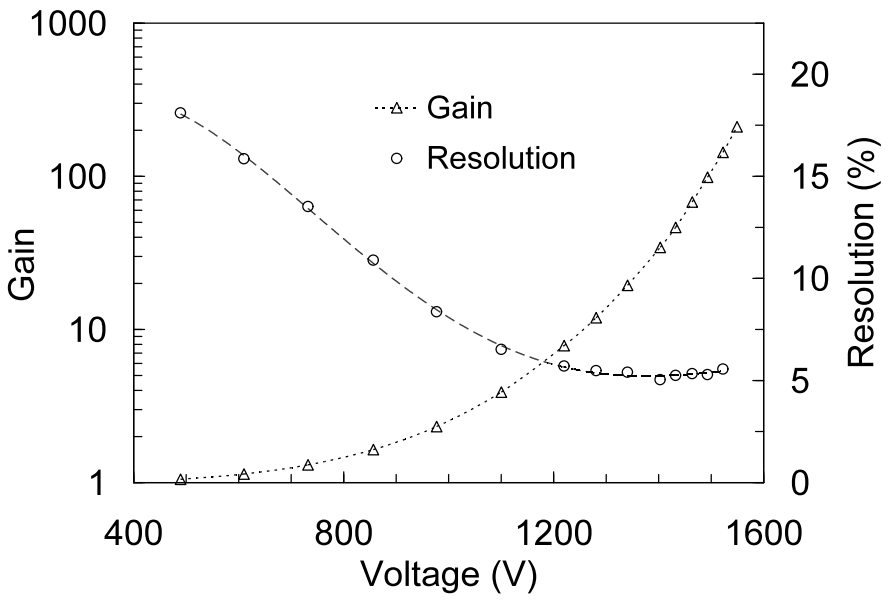

Fig. 3. Gain and energy resolution for scintillation pulses produced in LXe as a function of the APD bias voltage.

In this work, we use for *QE* the definition often found in the literature:

$$QE = \frac{\text{average number of electron-hole pairs produced in the APD } (N_e)}{\text{average number of photons reaching the APD } (N_{ph})} \qquad (1)$$

N_e can be determined by normalizing the scintillation signal amplitude, A_{UV}, to that resulting from direct interaction of alpha-particles in the APD, A_α, obtained at the same gain:

$$N_e = N_{e\alpha} \times \frac{A_{UV}}{A_\alpha} \qquad (2)$$

where $N_{e\alpha}$ is the number of charge carriers produced by alpha particles directly absorbed in the APD.

Figure 4 shows the pulse-height distributions for each case. The LAAPD was biased with 500V. At this voltage the gain is unitary independent of temperature, so the comparison is valid.

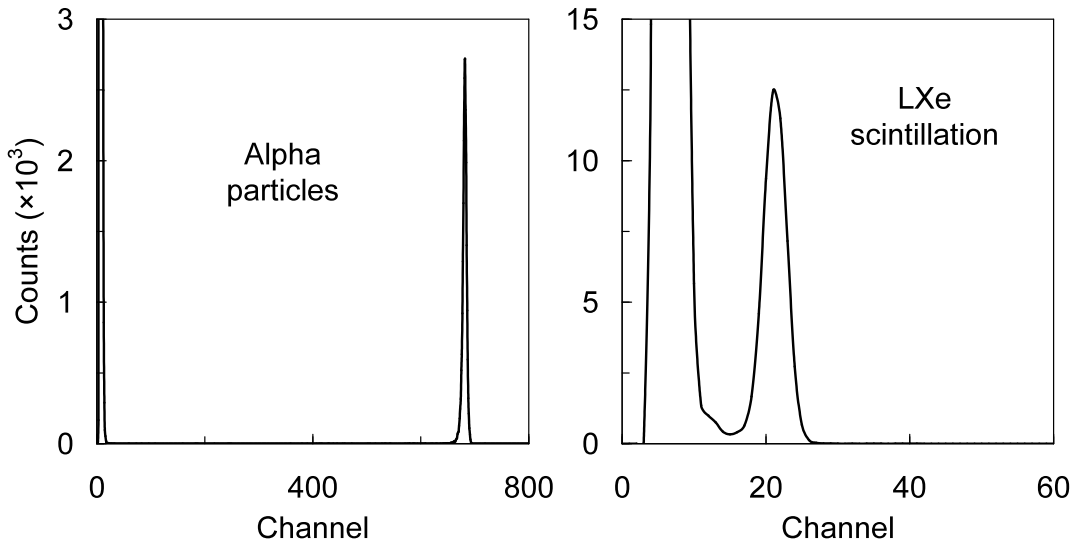

Fig. 4. Pulse-height distributions obtained from direct alpha particles (left) and LXe scintillation (right) measured with the API LAAPD at unitary gain (500V).

From Fig. 4 we obtain $A_{UV} = 21.25$ and $A_{\alpha} = 681.9$. $N_{e\alpha}$ is determined by the alpha particle energy, E_{α}, and the *w*-value in silicon (3.62 eV [11]):

$$N_{e\alpha} = \frac{E_{\alpha}}{w} = \frac{5.486\,\text{MeV}}{3.62\,\text{eV}} \cong 1.515 \times 10^{6}. \qquad (3)$$

Therefore, from Eq. (2) we obtain $N_e = 4.71 \times 10^4$ electron-hole pairs.

On the other hand, N_{ph} can be obtained from

$$N_{ph} = N_T \times \Omega_r \qquad (4)$$

where N_T is the total number of photons produced in LXe by an alpha-particle (on average) and Ω_r is the fraction of solid angle subtended by the APD. N_T is given by

$$N_T = \frac{5.486\,\text{MeV}}{19.6\,\text{eV}} \cong 2.80 \times 10^{5} \qquad (5)$$

since the average energy required to produce a photon in LXe for alpha particles is 19.6 eV [12].

For the API LAAPD the relative solid angle is $\Omega_r = 0.156$, so we obtain a quantum efficiency of 1.08±0.05. This value is in agreement with room temperature measurements [13,14] and with that reported for gas xenon scintillation light (~172 nm) [14], being 10% lower than that obtained for low pressure gas xenon scintillation light [8].

B) Hamamatsu APDs

In Fig. 5 we show typical pulse-height distributions obtained from direct alpha particles and LXe scintillation detected by the two Hamamatsu APDs.

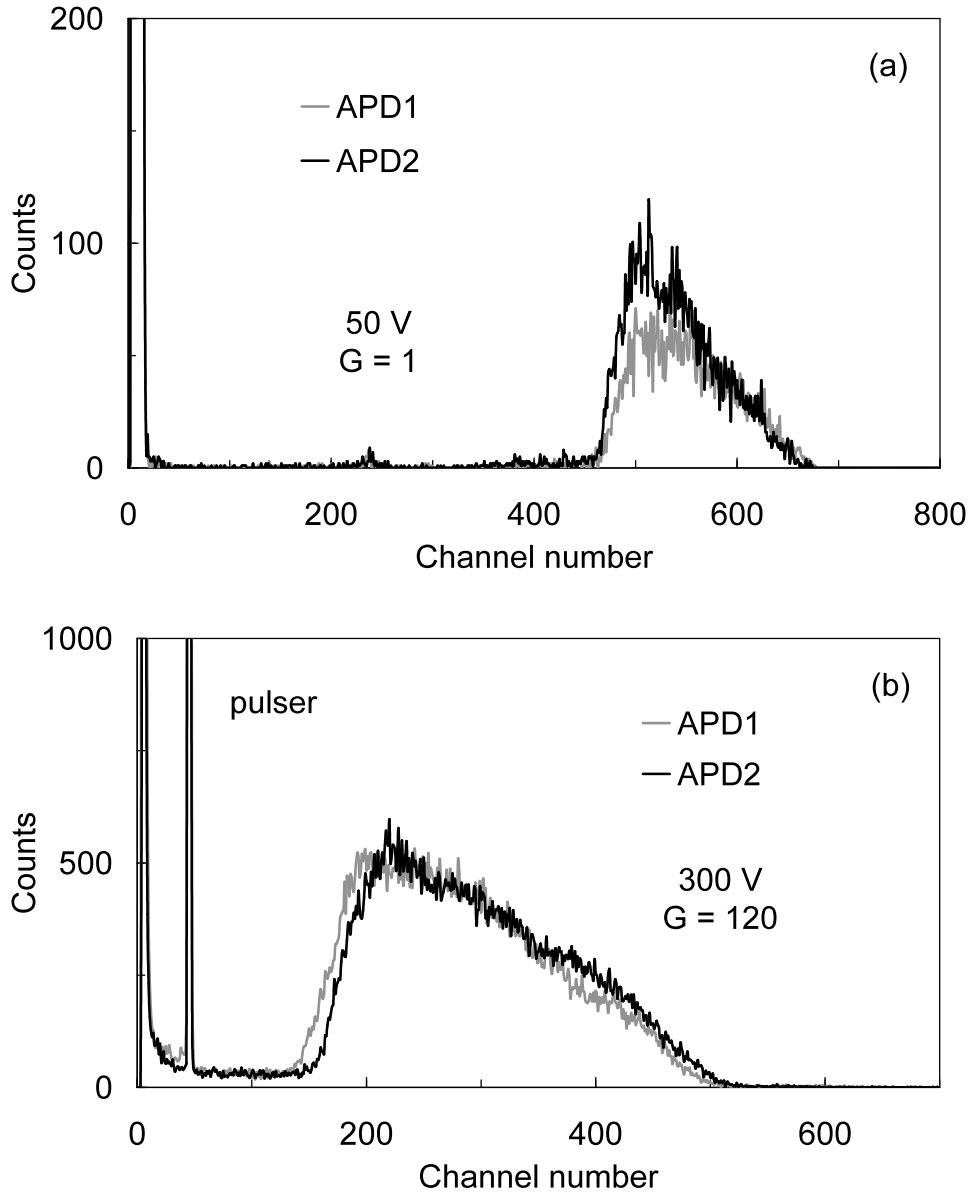

Fig. 5. Pulse-height distributions obtained from direct alpha particles (a) and LXe scintillation (b) detected in both the Hamamatsu APDs. Bias voltages of 50V and 300V were applied to the APDs for (a) and (b), respectively, corresponding to gains of 1 and 120.

The scintillation signals are significant compared to noise only for the highest gains. Both alpha particles and scintillation photons absorbed in the APDs lead to very

asymmetric pulse-height distributions with a significant tail towards the high-energy region. However, visible-light pulses emitted from a LED present Gaussian-shape pulse-height distributions. We attribute this effect to the difference in the average depth of photon interaction (about 1 μm and 5 nm for visible and 175 nm photons, respectively [15,16]). VUV photons interact mainly within the first few atomic layers, where the electric field is weaker. These factors result in higher diffusion of charge carriers that can be lost to the entrance electrode and impurities. Enhanced quantum efficiency in the VUV region is a result of maximizing the quantum yield and transmittance, while reducing recombination, through the selection of an optimized thickness of the entrance layer and the use of a suitable anti-reflection layer. The use of high-quality silicon also reduces losses from recombination of charge carriers.

The gain for Hamamatsu APDs was determined from LED pulses as they produce Gaussian peaks. Figure 6 shows the gain and energy resolution for the APDs as a function of the bias voltage. As shown, gains of a few hundred are achieved for bias voltages of a few hundred volts, a possible advantage when compared to the API APDs. The unitary gain was obtained for bias voltages of about 50 V and the best energy resolution was achieved for gains above 10.

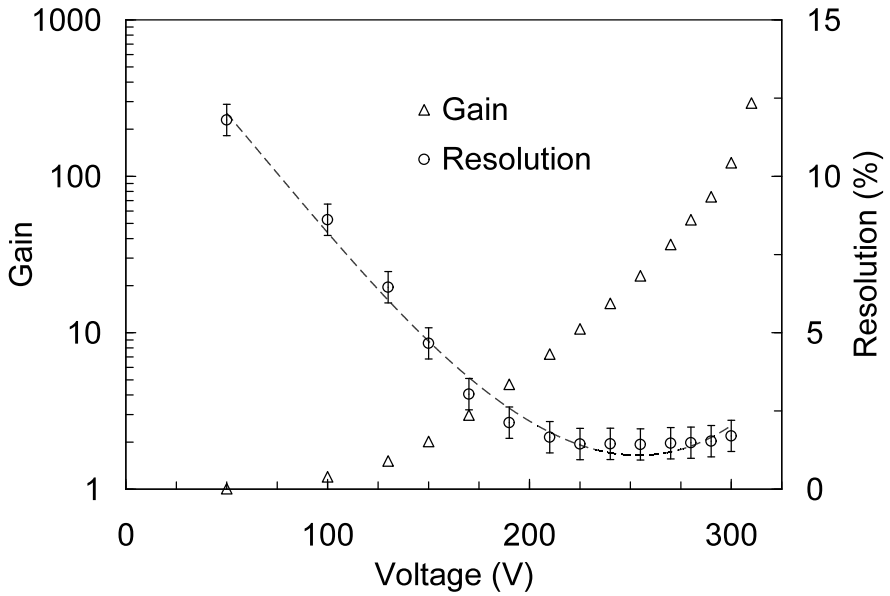

Fig. 6. Gain and energy resolution for visible-light pulses from a LED detected by a Hamamatsu APD, as a function of the APD bias voltage.

The quantum efficiency of the Hamamatsu APDs was determined using the procedure described in the previous section, using the data of Fig. 5. Peak positions were assumed to be given by fitting a Gaussian curve near the peak maximum. Since the centroid of the scintillation pulses could only be measured at high gains, the corresponding amplitude has to be normalized to the unitary gain. As mentioned before, the fraction of solid angle subtended by the APDs, relative to the alpha source, is $\Omega_r = 0.0235$. As before, $N_T \cong 2.80 \times 10^5$ and $N_{e_\alpha} \cong 1.515 \times 10^6$. We reach A_{UV}/A_α values of 3.39×10^{-3} and 3.59×10^{-3}, for APD1 and APD2, respectively, leading to *QE* values of 0.78±0.14 and 0.82±0.14. Our study demonstrates that the Hamamatsu APDs are sensitive at 178 nm, but we do not fully understand the reasons for their poor energy response

We have investigated the performance of API and Hamamatsu APDs for the detection of LXe scintillation while immersed in LXe. Quantum efficiencies of 1.08±0.05 and 0.80±0.14 where measured for the API and Hamamatsu APDs, respectively. Both APDs can reach gains of several hundred, but gains of as low as a few tens may be sufficient to achieve good energy resolution. The overall performance of the API APDs in LXe scintillation readout is superior. Not only do they present larger QE and larger active area, but also there is no peak distortion. Nevertheless, Hamamatsu APDs have also shown to be good candidates. Their performance would benefit from improved entrance layer design in order to reduce the observed peak distortions. The APD scintillation threshold in LXe remains yet to be addressed. This issue is crucial for dark matter search: the scintillation light resulting from a WIMP induced nuclear recoil of a few keV may not produce enough scintillation to be detected efficiently by the APD. Future work will explore this issue. On the other hand, other properties of the APDs such as their compact size, high *QE*, and compatibility with low radioactive background and LXe high purity requirements make them attractive for use in LXe detectors in particle physics, medical imaging and astrophysics applications.

Acknowledgements

This work was in part supported by DOE with Award DE-FG02-05ER41389 to the Columbia Astrophysics Laboratory.

References

[1] C.M.B. Monteiro, L.M.P. Fernandes, J.A.M. Lopes, J.F.C.A. Veloso, J.M.F. dos Santos, Appl. Phys. B **81** (2005) 531-535.

[2] M. Moszynski, M. Szawlowski, M. Kapusta and M. Balcerzyk, Nucl. Instr. Meth. A 497 (2003) 226.

[3] E. Aprile et al., The XENON Dark Matter Search Experiment: astro-ph/0207670.

[4] H.M. Araújo et al., the ZEPLIN-III dark matter detector: performance study using an end-to-end simulation tool, Astroparticle Physics **26** (2006) 140.

[5] EXO Experiment, see online http://www-project.slac.stanford.edu/exo/ (Phys. Rev. B 68 (2003) 054201).

[6] Advanced Photonix, Inc. (1240 Avenida Acaso, Camarillo, CA 93012, EUA), UV and Deep-UV series (http://www.advancedphotonix.com).

[7] V.N. Solovov et al., Nucl. Instr. Meth. A 488 (2002) 572.

[8] R. Chandrasekharan, M. Messina, A. Rubbia, Nucl. Instr. Meth. A 546 (2005) 426.

[9] K. Ni, E. Aprile, D. Day, K.L. Giboni, J.A.M. Lopes, P. Majewski, M. Yamashita, Nucl. Instr. Meth. A 551 (2005) 356.

[10] A. Hitachi et al., Phys. Rev. B 27 (1983) 5279.

[11] G.F. Knoll, Radiation Detection and Measurement, 3rd Edition, Wiley, New York, 2000.

[12] T. Doke, et al., Nucl. Instr. and Meth. A 420, 62-80 (1999).

[13] B. Zhou, M. Szawlowski, "An explanation on the APD spectral quantum efficiency in the deep UV range", Interoffice Memo, Advanced Photonix Inc., 1999.

[14] J.A.M. Lopes, J.M.F. dos Santos, R.E. Morgado, C.A.N. Conde, IEEE Trans. Nucl. Sci. 48 (2001) 312.

[15] K. Deiters, Y. Musienko, S. Nicol, B. Patel, D. Renker, S. Reucroft, R. Rusak, T. Sakhelashvilli, J. Swain, P. Vikas, Nucl. Instr. Meth. A 442 (2000) 193.

[16] T.W. Barnard, M.M.I. Crockett, J.C. Ivaldi, P.L. Lundberg, D.A. Yates, P.A. Levine, D.J. Sauer, Anal. Chem. 65 (1993) 1231.

Operation of Avalanche Photodiodes in Liquid Xenon

J. Alvarez, E. Aprile, K.L. Giboni, and L.M.P. Fernandes

Department of Physics, Columbia University, New York, NY 10027, USA

Columbia Astrophysics Laboratory Internal Report

Abstract

The operation of different avalanche photodiodes (APDs) for detection of liquid xenon scintillation was investigated. Quantum efficiencies of 1.08±0.05 and 0.80±0.14 where measured for two APD's provided by *Advanced Photonix Inc.* (API) and *Hamamatsu Photonics*, respectively. Both APD types were found to reach gains above 200, although gains as low as a few tens may prove sufficient to achieve optimum performance. Compared to the API photodiodes, the Hamamatsu APDs used in these tests exhibited poor performance.

I. Introduction

Avalanche photodiodes (APDs) have proven to be a good alternative to photomultiplier tubes (PMTs) in visible and VUV photon detection [1,2]. They are compact, consume small amounts of power, and are simple to operate. Operational characteristics such as high quantum efficiency, fair internal gain and insensitiveness to intense magnetic fields combined with a relatively low response to minimum ionizing particles make them competitive alternatives to PMTs for medium and high-energy physics instrumentation applications. In particular, their negligible radioactivity contamination is attractive for low background experiments based on liquid xenon (LXe), such as direct dark matter searches (XENON [3], ZEPLIN [4]) and the neutrinoless double beta decay search (EXO [5]), where the radio-purity of the photosensors is of critical importance. Their main drawbacks compared to PMTs are their low gains and reduced active areas

We have tested the operation of two types of APDs immersed in LXe. Until now, only API APDs *(Deep-UV series)* [6] presented a spectral response extending down to the VUV region (down to 120 nm). Another attractive quality from this perspective is the capability of to operate in direct contact with LXe (at -100 degrees C) with an estimated quantum efficiency (QE^1) of approximately 1 (as reported in [7]). High quantum efficiency for xenon gas scintillation (centred at 172 nm) was also reported to be about 1.2 [6] and 1.3 ± 0.1 [8]. In a previous work [9], we have used an API UV-series large area APD (LAAPD), mounted on a custom designed ceramic enclosure, and obtained a *QE* of 0.45 for the LXe scintillation (centred at 178 nm).

In this work, we summarize the results obtained with an API Deep-UV LAAPD, mounted in a custom designed ceramic enclosure, as well as with custom made Hamamatsu APDs with enhanced sensitivity in the VUV region. The measurements reported in this paper aim to confirm the high *QE* of the API LAAPD and to evaluate the *QE* of the Hamamatsu APDs at 178 nm, while immersed in LXe.

II. Experimental setup

The LAAPDs were mounted on a PTFE plate placed inside a chamber filled with high purity LXe. A negligibly small-sized ^{241}Am alpha source, deposited on the centre of a stainless steel plate, was placed above the LAAPD surface plane. A schematic drawing of the chamber is shown in Fig. 1. An open bath cooling apparatus with a liquid nitrogen (LN_2) and alcohol mixture was used to condense the xenon gas.

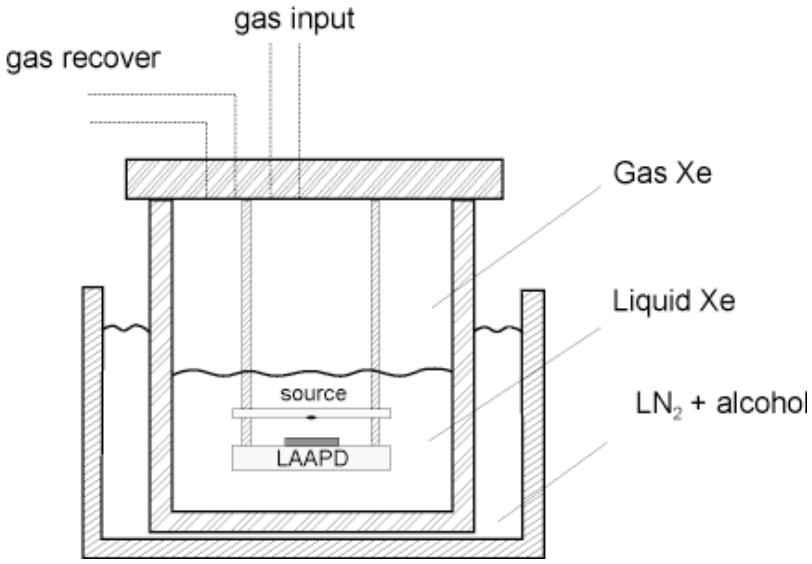

Fig. 1. LAAPD setup for scintillation detection in liquid xenon.

The scintillation light produced by alpha particles absorbed in LXe hits the LAAPD producing electron-hole pairs, which are amplified by avalanche in the silicon. The signal is collected in a charge sensitive preamplifier (*Canberra 2006*) and fed into a low-noise shaping amplifier (*Ortec 450*). Shaping time constants of 250 ns were used in order to optimize the APD performance for detection of the liquid xenon scintillation light, which has two scintillation components decaying at 4.2 ns and 22 ns [10]. The amplified signals are further pulse-height analysed in a multi-channel analyzer (MCA).

Two different types of APDs were tested in the chamber: a circular LAAPD (16 mm diameter) from API, placed in the centre of the PTFE disk, and two square shaped APDs (5×5 mm^2) from Hamamatsu Photonics, placed side by side in the centre of the PTFE plate. The distance between the source plane and the LAAPD surface was 7.5 mm and 6.5 mm for API and Hamamatsu APDs, respectively. With this geometry, the

relative solid angle subtended by the APDs (obtained from a MonteCarlo simulation), is 15.6% for the API LAAPD and 2.35% for each of the Hamamatsu APDs.

Manufacturer	**API**	**Hamamatsu**
Shape	circular, 10mm diam.	square, 5x5 mm^2
Distance from source plane	7.5mm	6.5mm
Fractional solid angle	15.6%	2.35%

The quantum efficiencies of the APDs were estimated by comparison of the VUV-scintillation pulse amplitudes with those resulting from direct interaction of the alpha particles in the photodiodes. The average number of charge carriers produced by alpha particles in the APD can be used as a reference to determine the number of charge carriers produced by the scintillation pulses. The pulse-height distributions from direct interaction of alpha particles in the APDs were obtained when the chamber was kept under vacuum.

III. Results and discussion

A) API LAAPD

Typical pulse-height distributions for direct alpha particles and LXe scintillation detected in the LAAPD are shown in Fig. 2 (a) and (b), respectively. The peaks resulting from direct interaction of alpha particles present a Gaussian shape with negligible tails in the low energy region. This behavior is consistent with the negligible energy loss of the alpha particles in the APD entrance dead layer; alpha particles impinging the APD at different angles lead to essentially the same energy absorbed in the APD.

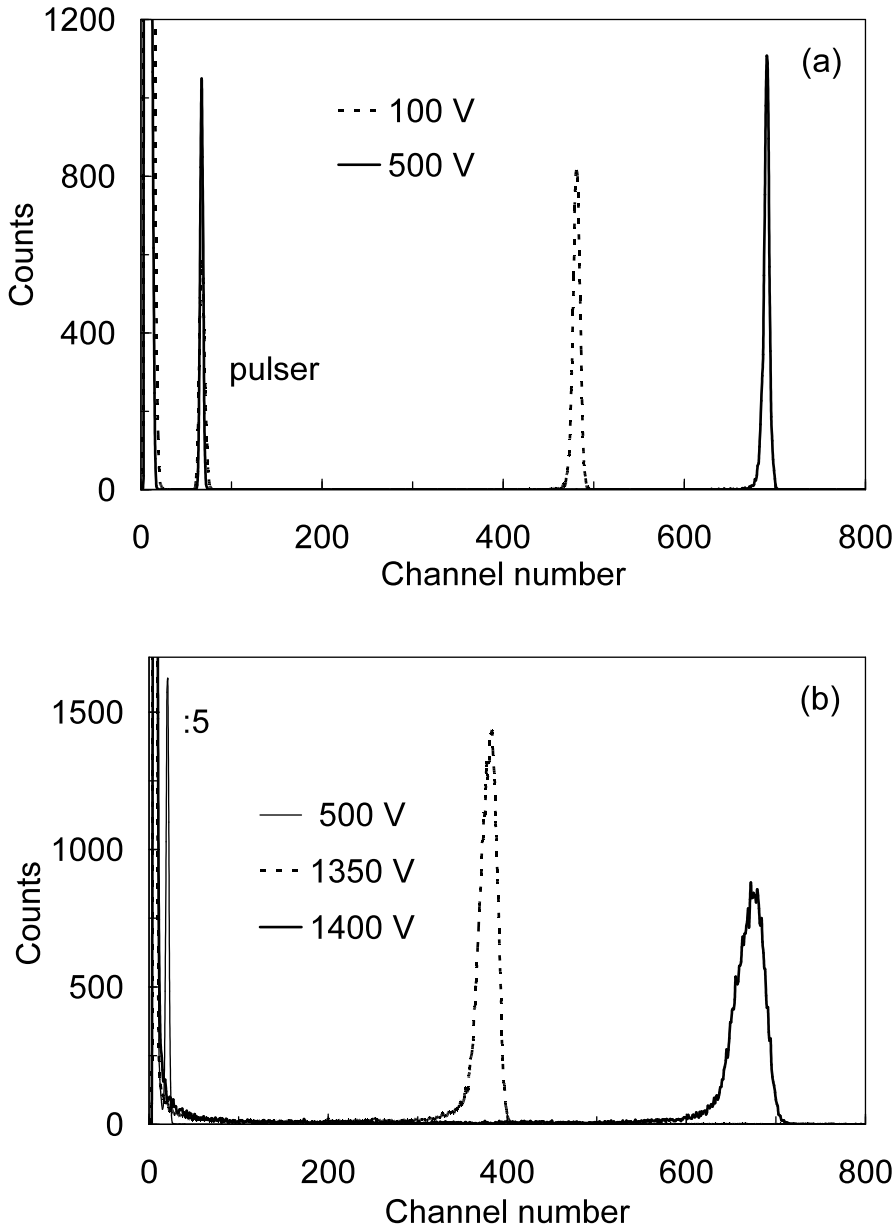

Fig. 2. Pulse-height distributions for direct alpha particles (a) and LXe scintillation (b) detected in the API LAAPD for different bias voltages. For higher bias voltages, alpha particle signals saturate the APD.

Fig. 3 shows the APD gain and energy resolution as a function of APD bias voltage, determined from the pulse-height distributions obtained for VUV scintillation produced in LXe by alpha particles. The unitary gain was obtained for a range of bias voltages around 500 V and is in accordance with the measurements made for visible light pulses from a LED. As shown in Fig. 3, the lowest energy resolution of 5.0% is obtained for gains above 35.

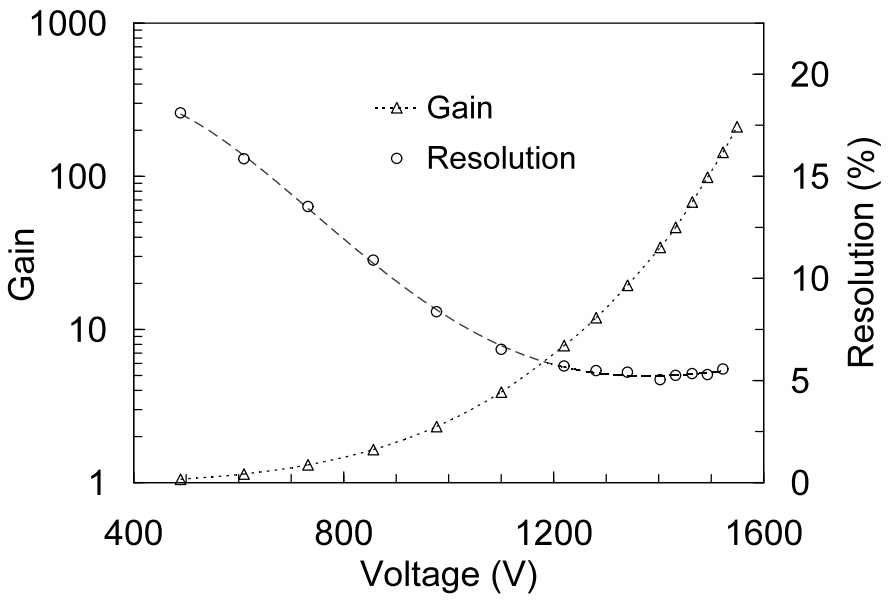

Fig. 3. Gain and energy resolution for scintillation pulses produced in LXe as a function of the APD bias voltage.

In this work, we use for *QE* the definition often found in the literature:

$$QE = \frac{\text{average number of electron-hole pairs produced in the APD } (N_e)}{\text{average number of photons reaching the APD } (N_{ph})} \qquad (1)$$

N_e can be determined by normalizing the scintillation signal amplitude, A_{UV}, to that resulting from direct interaction of alpha-particles in the APD, A_α, obtained at the same gain:

$$N_e = N_{e\alpha} \times \frac{A_{UV}}{A_\alpha} \qquad (2)$$

where $N_{e\alpha}$ is the number of charge carriers produced by alpha particles directly absorbed in the APD.

Figure 4 shows the pulse-height distributions for each case. The LAAPD was biased with 500V. At this voltage the gain is unitary independent of temperature, so the comparison is valid.

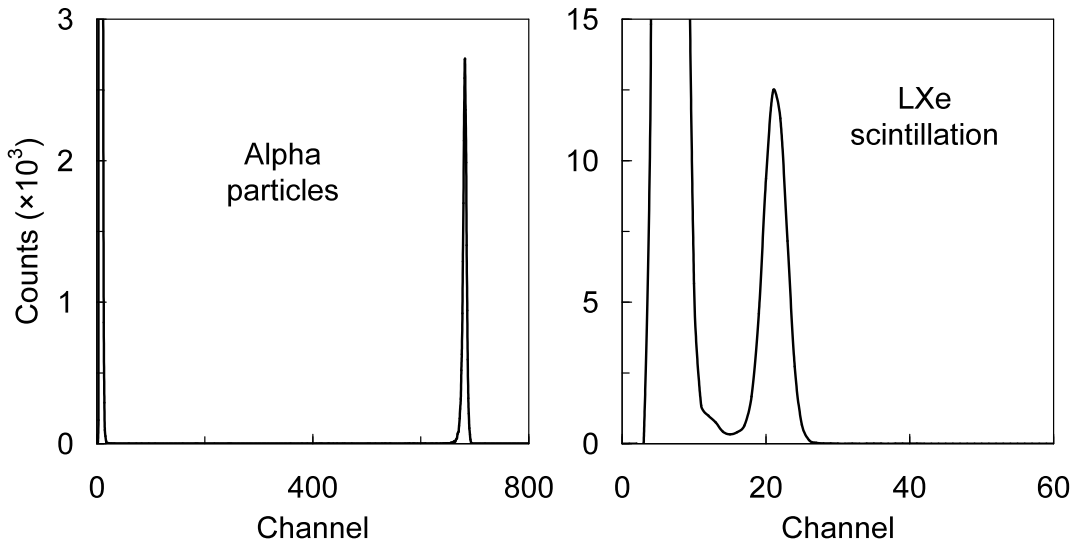

Fig. 4. Pulse-height distributions obtained from direct alpha particles (left) and LXe scintillation (right) measured with the API LAAPD at unitary gain (500V).

From Fig. 4 we obtain $A_{UV} = 21.25$ and $A_{\alpha} = 681.9$. $N_{e\alpha}$ is determined by the alpha particle energy, E_{α}, and the *w*-value in silicon (3.62 eV [11]):

$$N_{e\alpha} = \frac{E_{\alpha}}{w} = \frac{5.486\,\text{MeV}}{3.62\,\text{eV}} \cong 1.515 \times 10^{6}. \qquad (3)$$

Therefore, from Eq. (2) we obtain $N_e = 4.71 \times 10^4$ electron-hole pairs.

On the other hand, N_{ph} can be obtained from

$$N_{ph} = N_T \times \Omega_r \qquad (4)$$

where N_T is the total number of photons produced in LXe by an alpha-particle (on average) and Ω_r is the fraction of solid angle subtended by the APD. N_T is given by

$$N_T = \frac{5.486\,\text{MeV}}{19.6\,\text{eV}} \cong 2.80 \times 10^{5} \qquad (5)$$

since the average energy required to produce a photon in LXe for alpha particles is 19.6 eV [12].

For the API LAAPD the relative solid angle is $\Omega_r = 0.156$, so we obtain a quantum efficiency of 1.08±0.05. This value is in agreement with room temperature measurements [13,14] and with that reported for gas xenon scintillation light (~172 nm) [14], being 10% lower than that obtained for low pressure gas xenon scintillation light [8].

B) Hamamatsu APDs

In Fig. 5 we show typical pulse-height distributions obtained from direct alpha particles and LXe scintillation detected by the two Hamamatsu APDs.

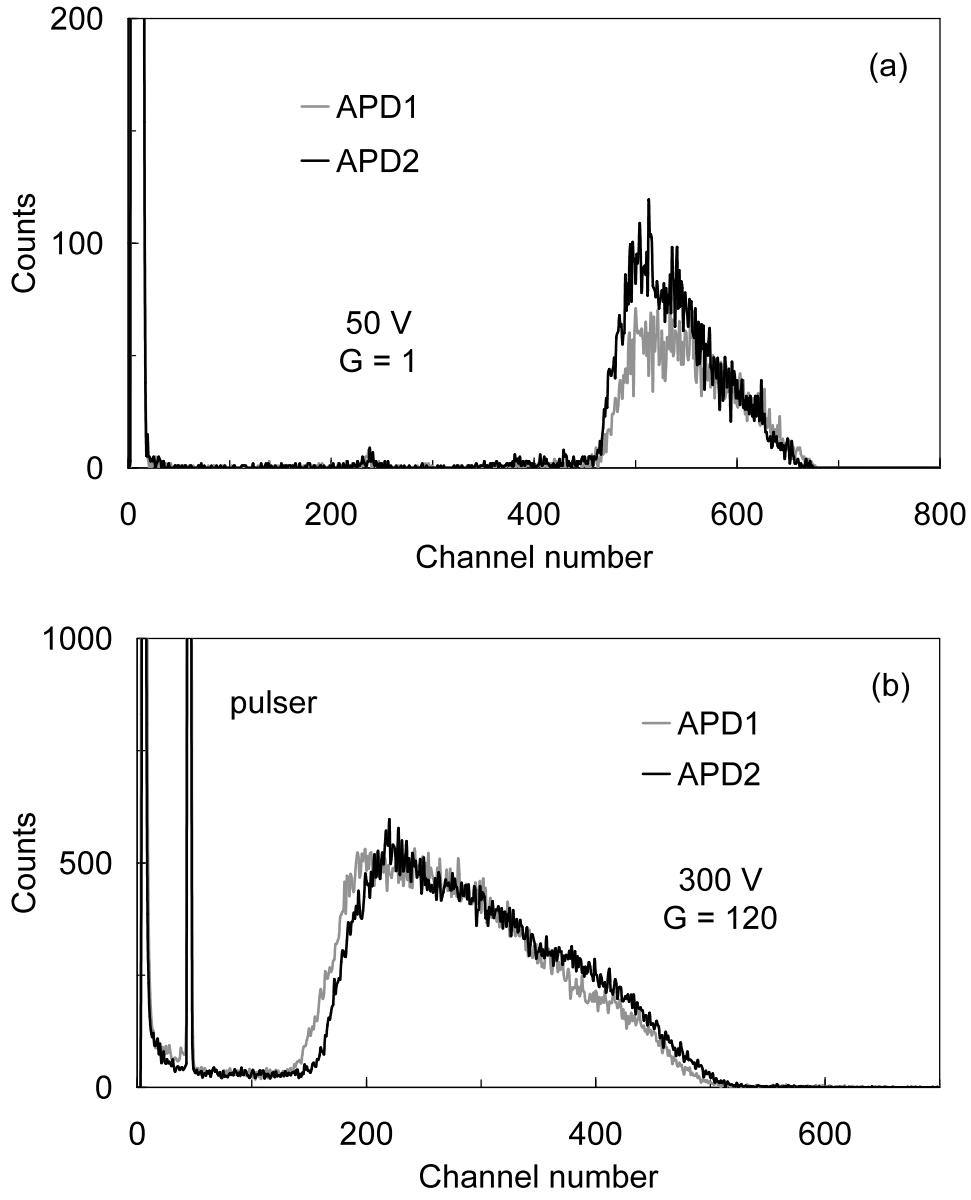

Fig. 5. Pulse-height distributions obtained from direct alpha particles (a) and LXe scintillation (b) detected in both the Hamamatsu APDs. Bias voltages of 50V and 300V were applied to the APDs for (a) and (b), respectively, corresponding to gains of 1 and 120.

The scintillation signals are significant compared to noise only for the highest gains. Both alpha particles and scintillation photons absorbed in the APDs lead to very

asymmetric pulse-height distributions with a significant tail towards the high-energy region. However, visible-light pulses emitted from a LED present Gaussian-shape pulse-height distributions. We attribute this effect to the difference in the average depth of photon interaction (about 1 μm and 5 nm for visible and 175 nm photons, respectively [15,16]). VUV photons interact mainly within the first few atomic layers, where the electric field is weaker. These factors result in higher diffusion of charge carriers that can be lost to the entrance electrode and impurities. Enhanced quantum efficiency in the VUV region is a result of maximizing the quantum yield and transmittance, while reducing recombination, through the selection of an optimized thickness of the entrance layer and the use of a suitable anti-reflection layer. The use of high-quality silicon also reduces losses from recombination of charge carriers.

The gain for Hamamatsu APDs was determined from LED pulses as they produce Gaussian peaks. Figure 6 shows the gain and energy resolution for the APDs as a function of the bias voltage. As shown, gains of a few hundred are achieved for bias voltages of a few hundred volts, a possible advantage when compared to the API APDs. The unitary gain was obtained for bias voltages of about 50 V and the best energy resolution was achieved for gains above 10.

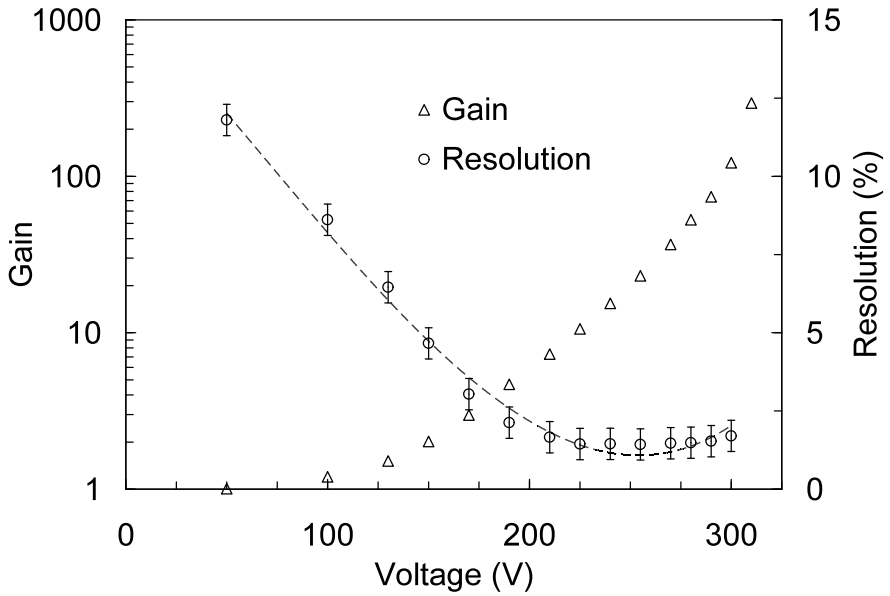

Fig. 6. Gain and energy resolution for visible-light pulses from a LED detected by a Hamamatsu APD, as a function of the APD bias voltage.

The quantum efficiency of the Hamamatsu APDs was determined using the procedure described in the previous section, using the data of Fig. 5. Peak positions were assumed to be given by fitting a Gaussian curve near the peak maximum. Since the centroid of the scintillation pulses could only be measured at high gains, the corresponding amplitude has to be normalized to the unitary gain. As mentioned before, the fraction of solid angle subtended by the APDs, relative to the alpha source, is $\Omega_r = 0.0235$. As before, $N_T \cong 2.80 \times 10^5$ and $N_{e_\alpha} \cong 1.515 \times 10^6$. We reach A_{UV}/A_α values of 3.39×10^{-3} and 3.59×10^{-3}, for APD1 and APD2, respectively, leading to *QE* values of 0.78±0.14 and 0.82±0.14. Our study demonstrates that the Hamamatsu APDs are sensitive at 178 nm, but we do not fully understand the reasons for their poor energy response

We have investigated the performance of API and Hamamatsu APDs for the detection of LXe scintillation while immersed in LXe. Quantum efficiencies of 1.08±0.05 and 0.80±0.14 where measured for the API and Hamamatsu APDs, respectively. Both APDs can reach gains of several hundred, but gains of as low as a few tens may be sufficient to achieve good energy resolution. The overall performance of the API APDs in LXe scintillation readout is superior. Not only do they present larger QE and larger active area, but also there is no peak distortion. Nevertheless, Hamamatsu APDs have also shown to be good candidates. Their performance would benefit from improved entrance layer design in order to reduce the observed peak distortions. The APD scintillation threshold in LXe remains yet to be addressed. This issue is crucial for dark matter search: the scintillation light resulting from a WIMP induced nuclear recoil of a few keV may not produce enough scintillation to be detected efficiently by the APD. Future work will explore this issue. On the other hand, other properties of the APDs such as their compact size, high *QE*, and compatibility with low radioactive background and LXe high purity requirements make them attractive for use in LXe detectors in particle physics, medical imaging and astrophysics applications.

Acknowledgements

This work was in part supported by DOE with Award DE-FG02-05ER41389 to the Columbia Astrophysics Laboratory.

References

[1] C.M.B. Monteiro, L.M.P. Fernandes, J.A.M. Lopes, J.F.C.A. Veloso, J.M.F. dos Santos, Appl. Phys. B **81** (2005) 531-535.

[2] M. Moszynski, M. Szawlowski, M. Kapusta and M. Balcerzyk, Nucl. Instr. Meth. A 497 (2003) 226.

[3] E. Aprile et al., The XENON Dark Matter Search Experiment: astro-ph/0207670.

[4] H.M. Araújo et al., the ZEPLIN-III dark matter detector: performance study using an end-to-end simulation tool, Astroparticle Physics **26** (2006) 140.

[5] EXO Experiment, see online http://www-project.slac.stanford.edu/exo/ (Phys. Rev. B 68 (2003) 054201).

[6] Advanced Photonix, Inc. (1240 Avenida Acaso, Camarillo, CA 93012, EUA), UV and Deep-UV series (http://www.advancedphotonix.com).

[7] V.N. Solovov et al., Nucl. Instr. Meth. A 488 (2002) 572.

[8] R. Chandrasekharan, M. Messina, A. Rubbia, Nucl. Instr. Meth. A 546 (2005) 426.

[9] K. Ni, E. Aprile, D. Day, K.L. Giboni, J.A.M. Lopes, P. Majewski, M. Yamashita, Nucl. Instr. Meth. A 551 (2005) 356.

[10] A. Hitachi et al., Phys. Rev. B 27 (1983) 5279.

[11] G.F. Knoll, Radiation Detection and Measurement, 3rd Edition, Wiley, New York, 2000.

[12] T. Doke, et al., Nucl. Instr. and Meth. A 420, 62-80 (1999).

[13] B. Zhou, M. Szawlowski, "An explanation on the APD spectral quantum efficiency in the deep UV range", Interoffice Memo, Advanced Photonix Inc., 1999.

[14] J.A.M. Lopes, J.M.F. dos Santos, R.E. Morgado, C.A.N. Conde, IEEE Trans. Nucl. Sci. 48 (2001) 312.

[15] K. Deiters, Y. Musienko, S. Nicol, B. Patel, D. Renker, S. Reucroft, R. Rusak, T. Sakhelashvilli, J. Swain, P. Vikas, Nucl. Instr. Meth. A 442 (2000) 193.

[16] T.W. Barnard, M.M.I. Crockett, J.C. Ivaldi, P.L. Lundberg, D.A. Yates, P.A. Levine, D.J. Sauer, Anal. Chem. 65 (1993) 1231.

Summary

Test of the SiPM at the Columbia Astrophysics Laboratory

SiPM

alpha source in

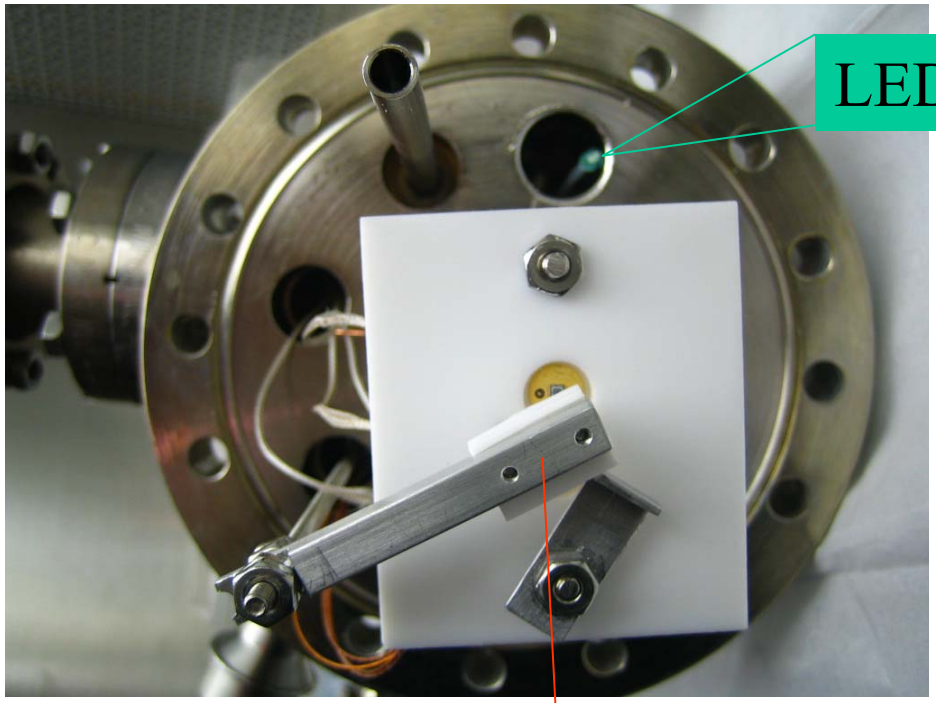

α-source: ^{210}Po

0.1 µCi @ 138.4d

alpha source out

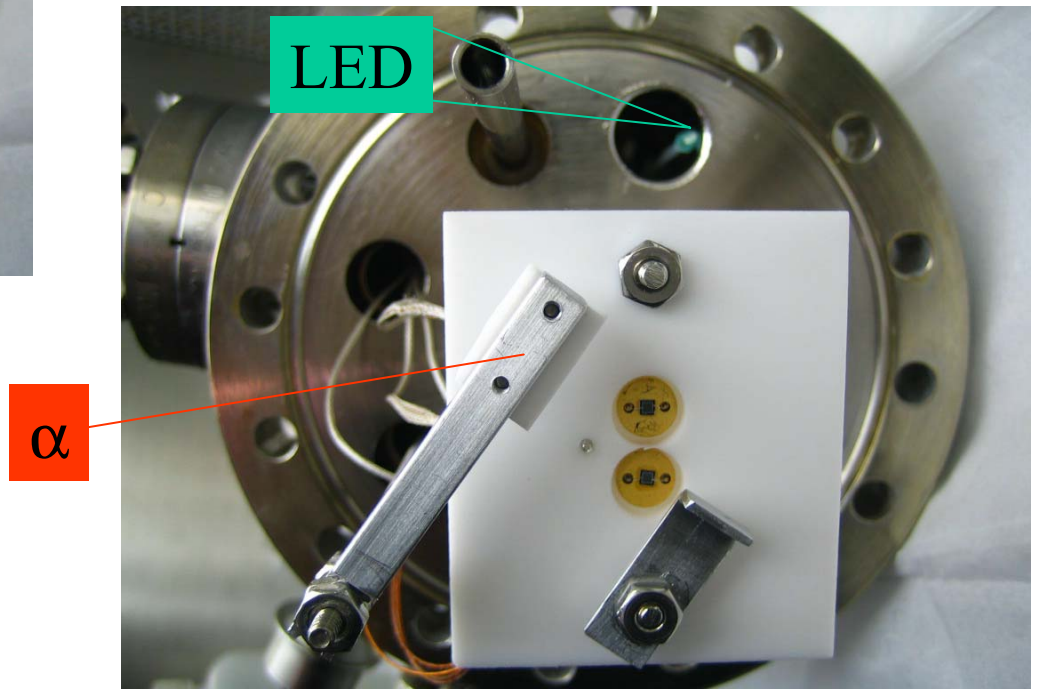

SiPM – Energy spectra with a gate requiring a signal in both PMTs of an alpha source in LXe

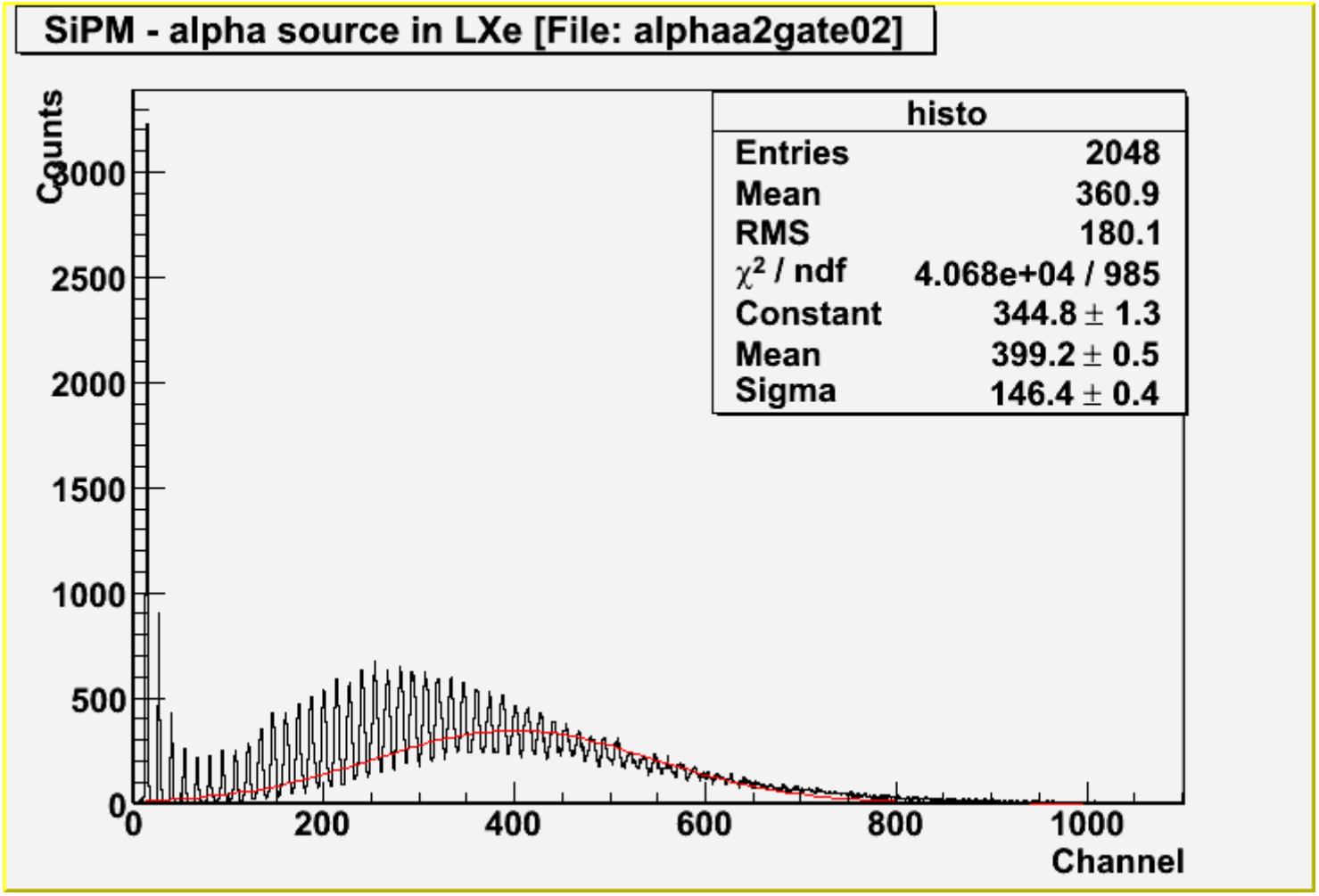

Signal from the anode 2 (Bias Voltage = -66.5V)

SiPM – Energy spectra with a gate requiring a signal in both PMTs of an alpha source in LXe

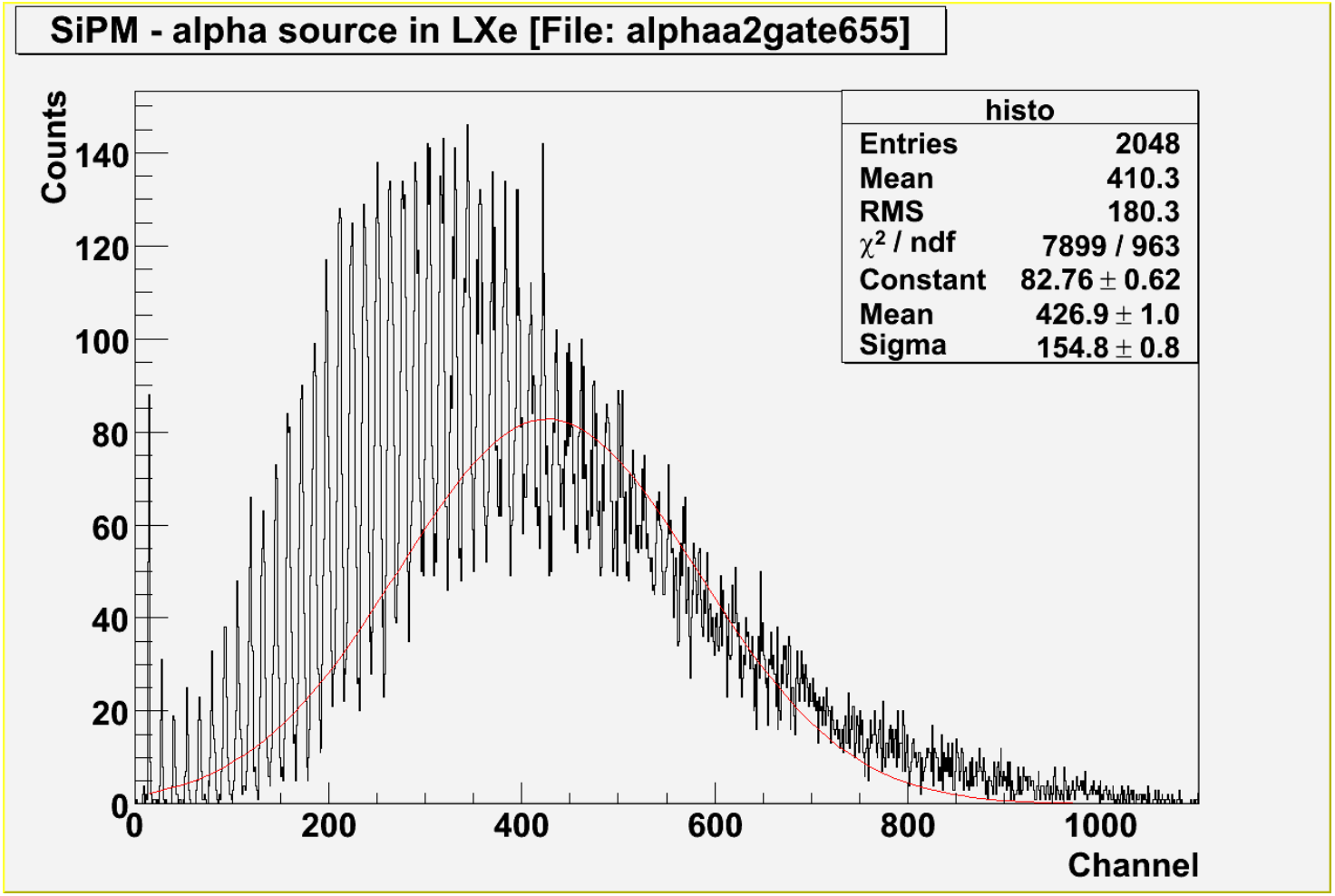

Signal from the anode 2 (Bias Voltage = -65.5V)

SiPM – Energy spectra with a gate requiring a signal in both PMTs of an alpha source in LXe

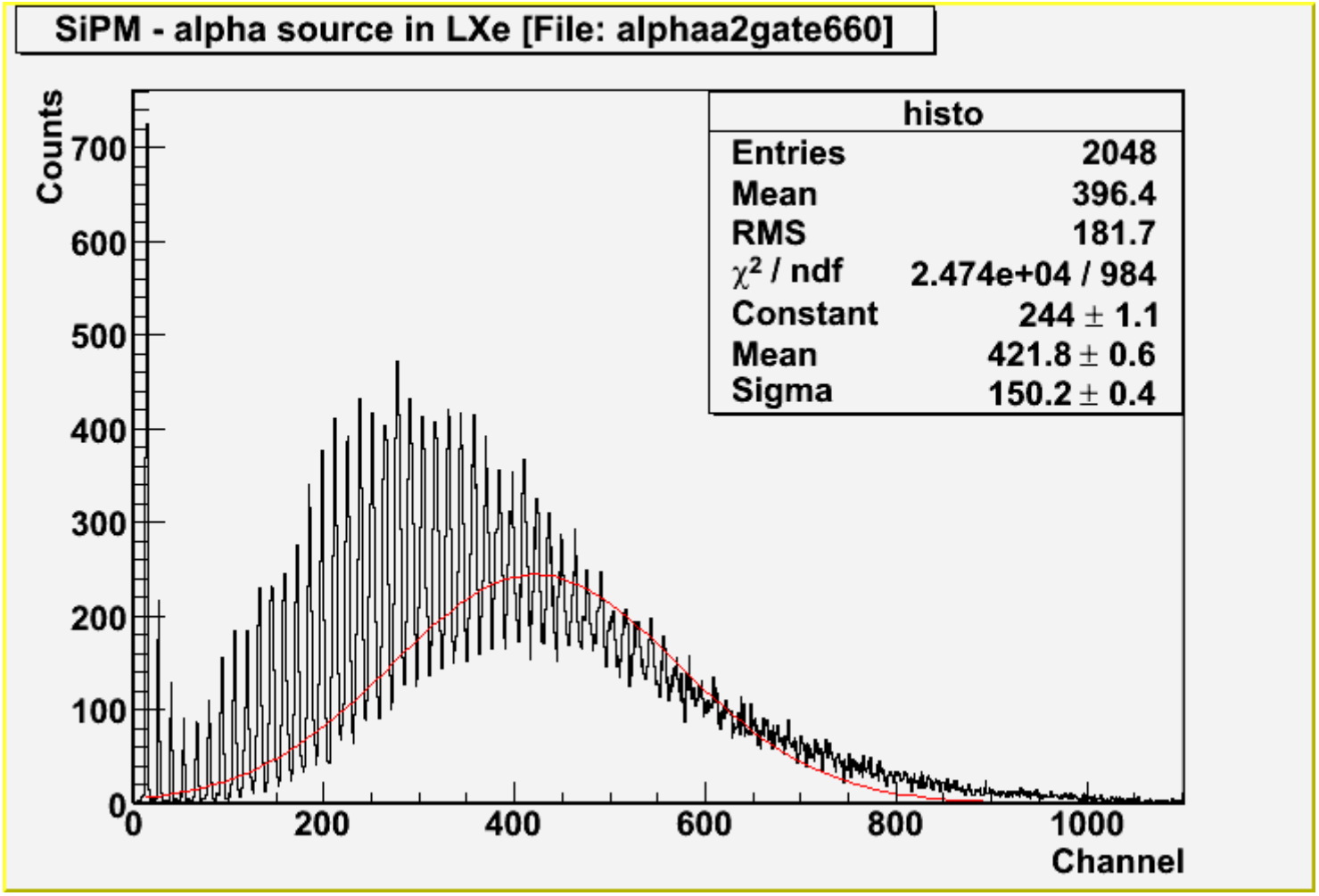

Signal from the anode 2 (Bias Voltage = -66.0V)

SiPM – Energy spectra with a gate requiring a signal in both PMTs of an alpha source in LXe

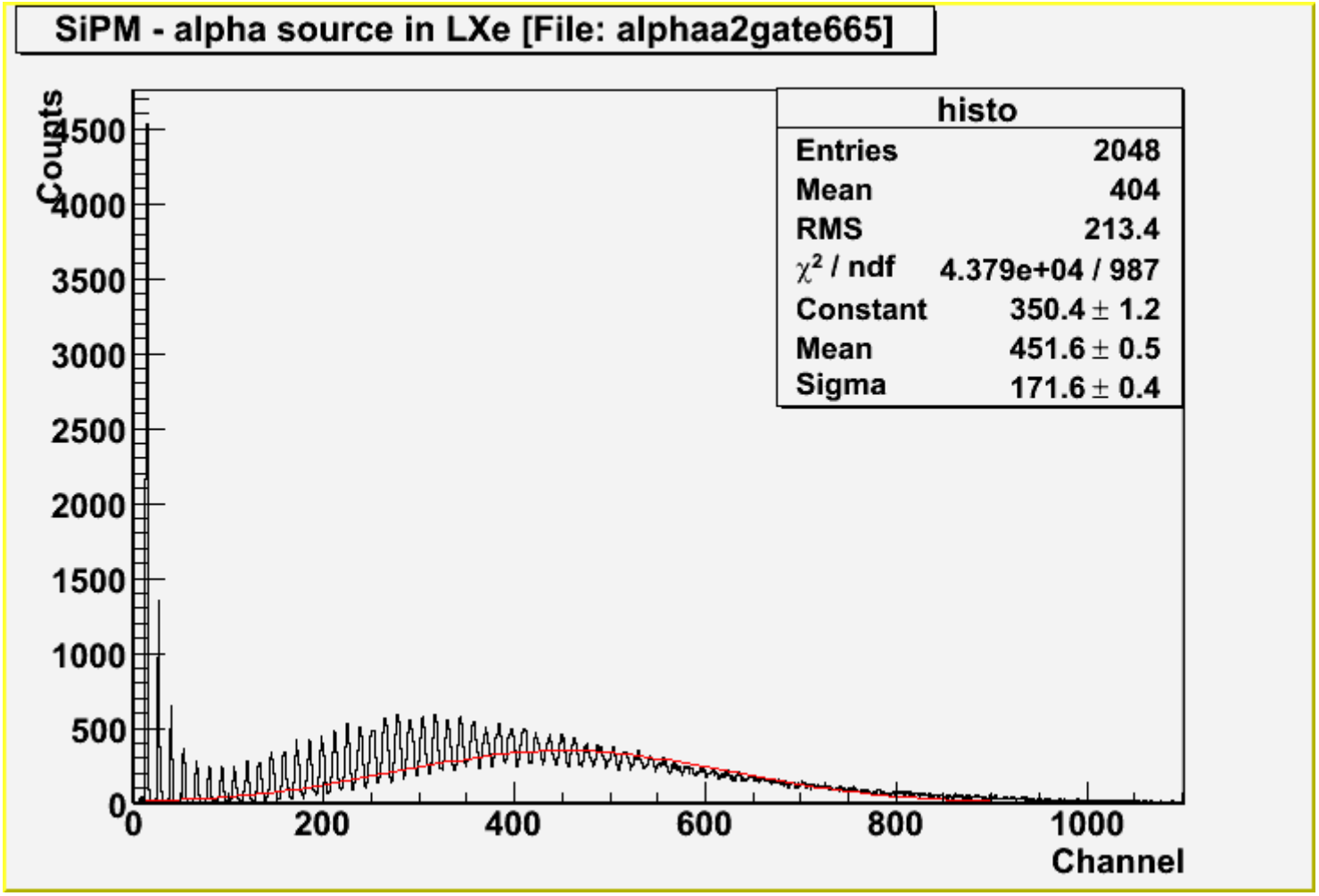

Signal from the anode 2 (Bias Voltage = -66.5V)

SiPM – Energy spectra with a gate requiring a signal in both PMTs of an alpha source in LXe

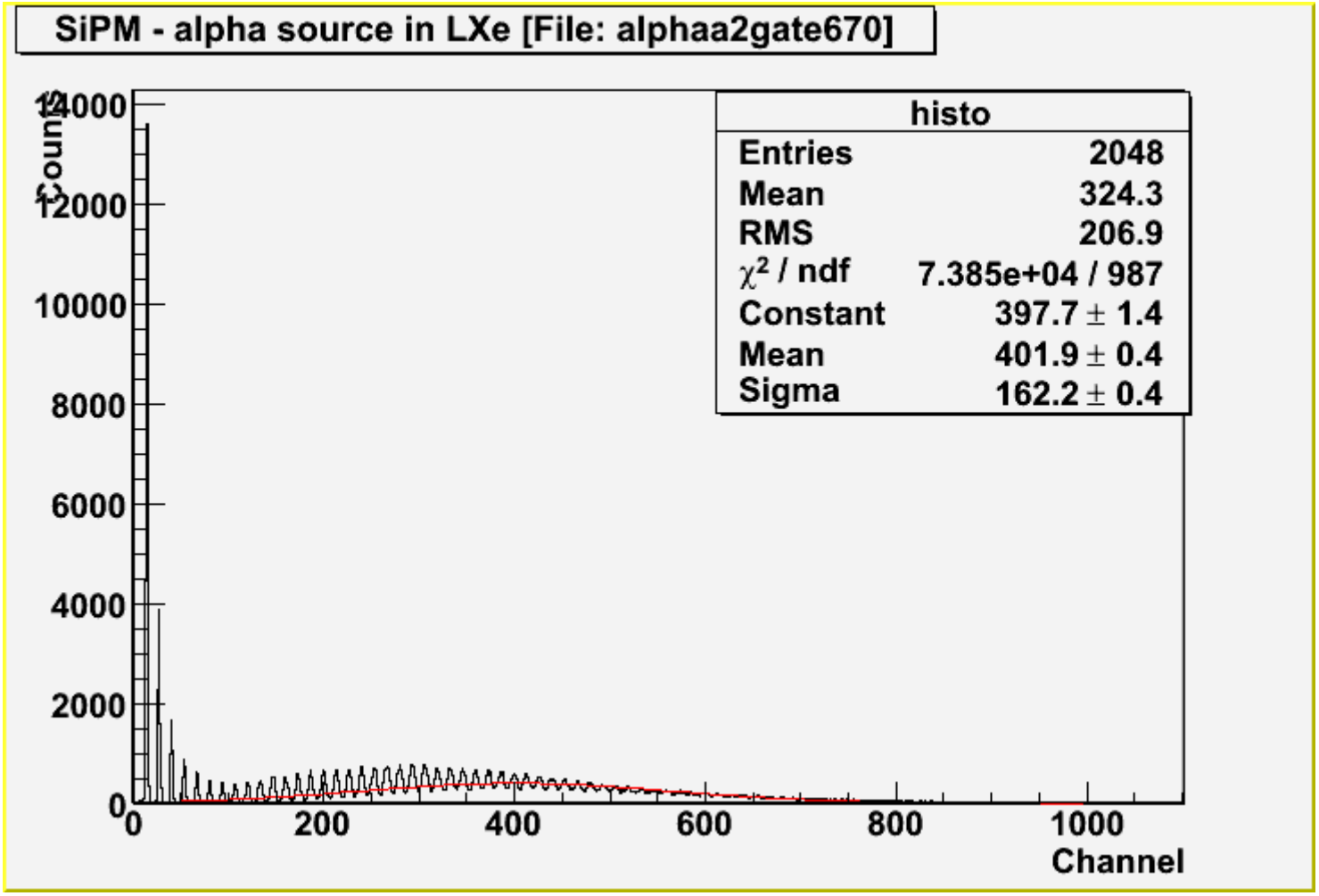

Signal from the anode 2 (Bias Voltage = -67.0V)

SiPM – Energy spectra with a gate requiring a signal in both PMTs of an alpha source in LXe

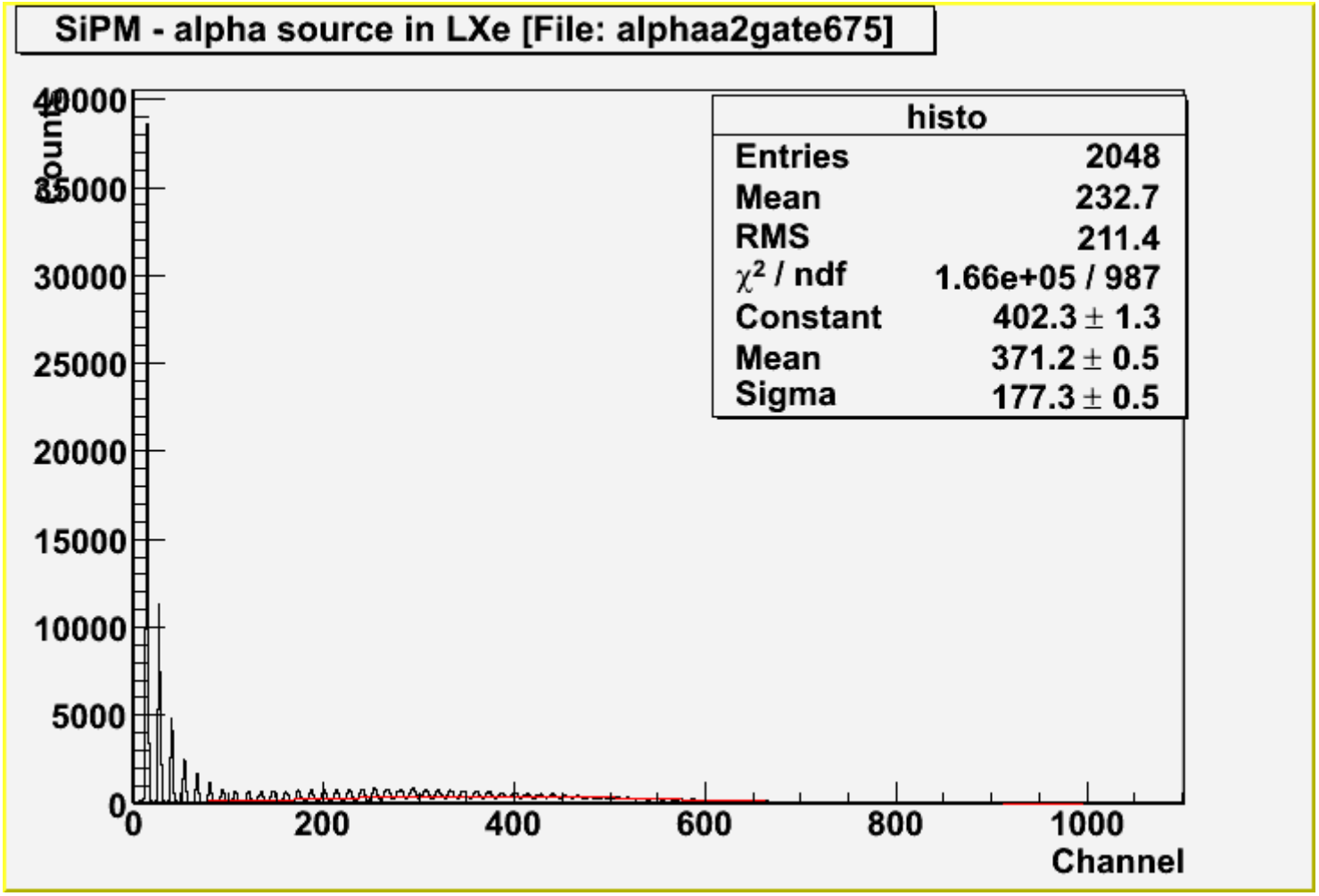

Signal from the anode 2 (Bias Voltage = -67.5V)

SiPM – Energy spectra with a gate requiring a signal in both PMTs of an alpha source in LXe

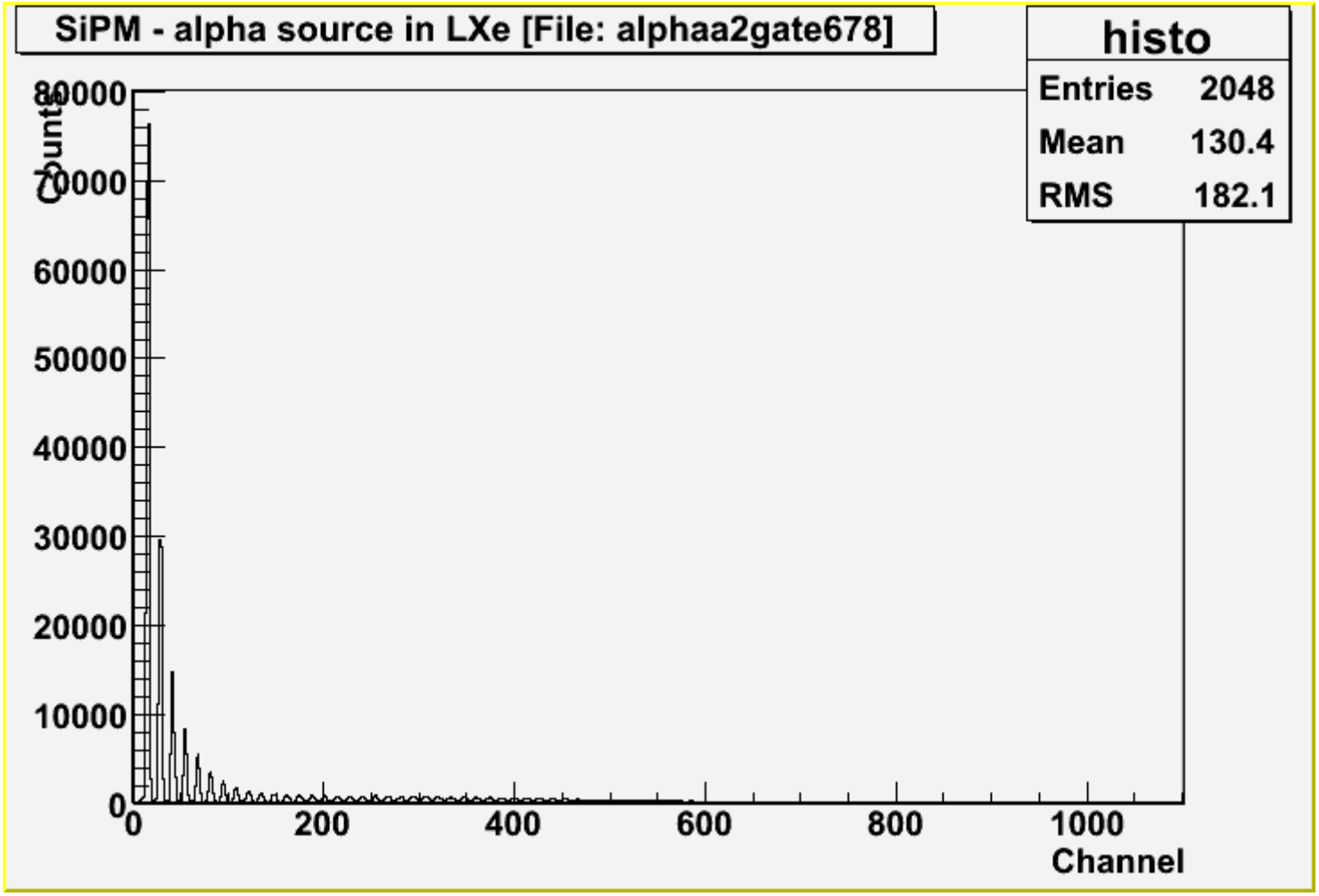

Signal from the anode 2 (Bias Voltage = -67.8V)

SiPM – Energy spectra with a gate requiring a signal in both PMTs of an alpha source in LXe

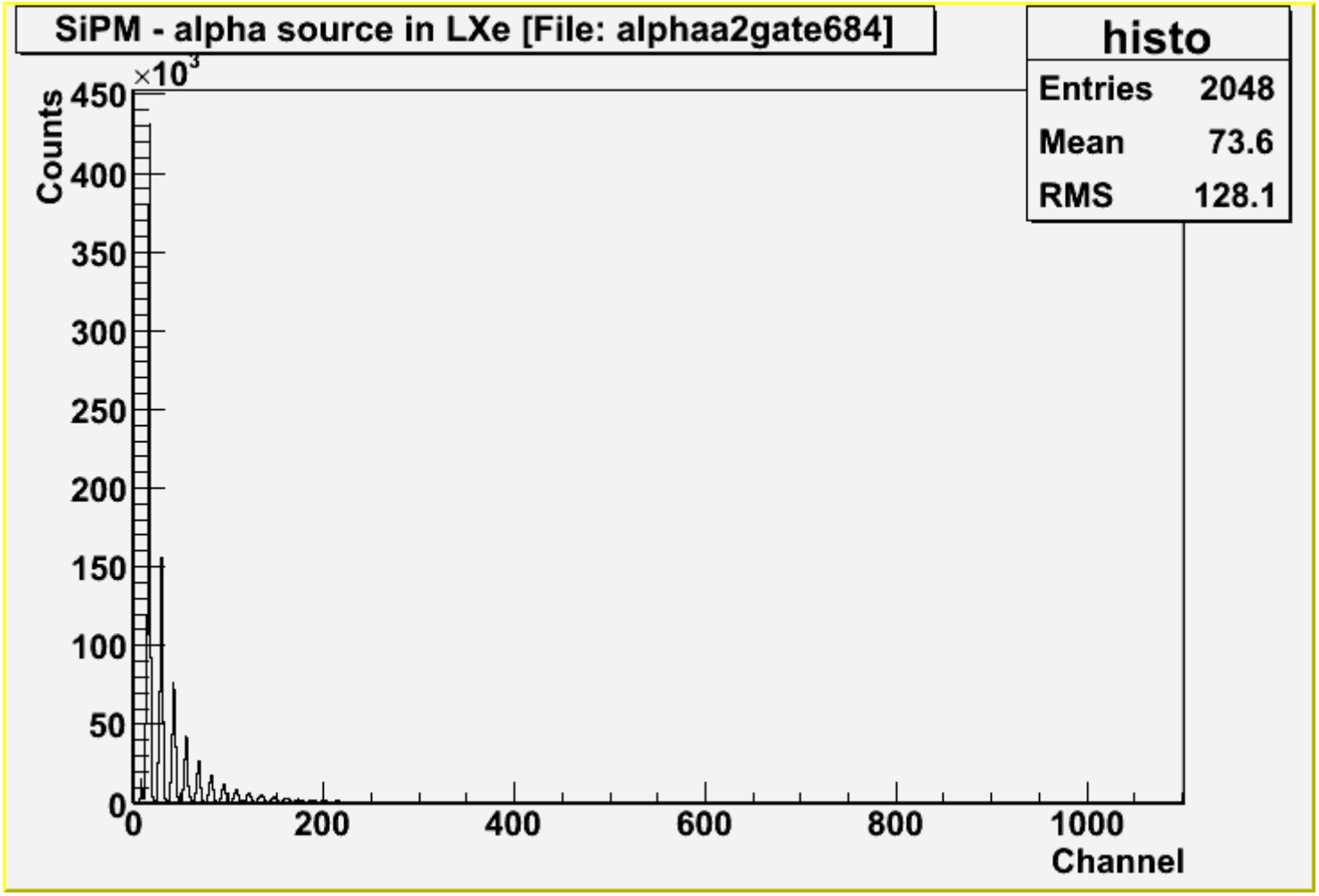

Signal from the anode 2 (Bias Voltage = -68.4V)

SiPM – Energy spectra with a gate requiring a signal in both PMTs of an alpha source in LXe

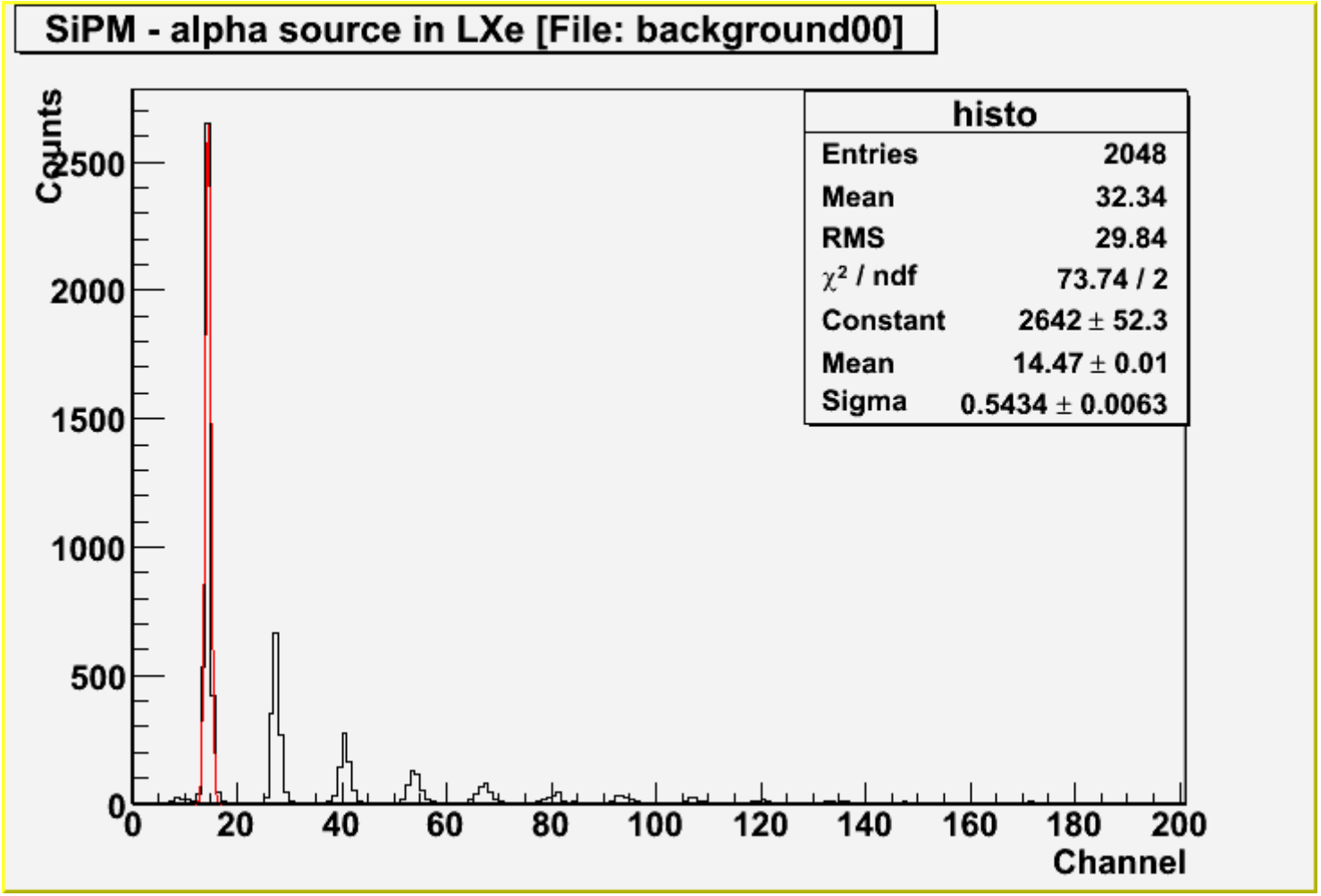

SiPM – Energy spectra with a gate requiring a signal in both PMTs of an alpha source in LXe